

# On the theory of the reaction rate of vibrationally excited CO molecules with OH radicals

Wei-Chen Chen and R. A. Marcus<sup>a)</sup>

Noyes Laboratory 127-72, California Institute of Technology, Pasadena, California 91125

(Received 13 October 2005; accepted 10 November 2005; published online 10 January 2006)

The dependence of the rate of the reaction  $\text{CO} + \text{OH} \rightarrow \text{H} + \text{CO}_2$  on the CO-vibrational excitation is treated here theoretically. Both the Rice-Ramsperger-Kassel-Marcus (RRKM) rate constant  $k_{\text{RRKM}}$  and a nonstatistical modification  $k_{\text{non}}$  [W.-C. Chen and R. A. Marcus, *J. Chem. Phys.* **123**, 094307 (2005).] are used in the analysis. The experimentally measured rate constant shows an apparent (large error bars) decrease with increasing CO-vibrational temperature  $T_v$  over the range of  $T_v$ 's studied, 298–1800 K. Both  $k_{\text{RRKM}}(T_v)$  and  $k_{\text{non}}(T_v)$  show the same trend over the  $T_v$ -range studied, but the  $k_{\text{non}}(T_v)$  vs  $T_v$  plot shows a larger effect. The various trends can be understood in simple terms. The calculated rate constant  $k^v$  decreases with increasing CO vibrational quantum number  $v$ , on going from  $v=0$  to  $v=1$ , by factors of 1.5 and 3 in the RRKM and nonstatistical calculations, respectively. It then increases when  $v$  is increased further. These results can be regarded as a prediction when  $v$  state-selected rate constants become available. © 2006 American Institute of Physics. [DOI: 10.1063/1.2148408]

## I. INTRODUCTION

The conversion of CO to  $\text{CO}_2$  by reaction with an OH radical is one of the principal oxidation reactions in the atmosphere<sup>1</sup> and has been the subject of many experimental<sup>2–16</sup> and theoretical studies.<sup>16–28</sup> The currently accepted reaction mechanism involves a CO and OH bimolecular association to form a vibrationally excited *trans*-HOCO\* radical, followed by a *cis-trans* isomerization. There are also the back reaction to reform the reactants, the forward reaction leading to  $\text{H} + \text{CO}_2$  and the collisional stabilization of HOCO\*. In the presence of oxygen both the  $\text{H} + \text{CO}_2$  and the stabilized HOCO form the same products,  $\text{HO}_2$  and  $\text{CO}_2$ .<sup>29–31</sup>

The non-Arrhenius behavior for the thermal rate constant has been extensively studied in experiments and theory.<sup>3–12,16,20,21,26–28</sup> It involves a nearly activationless barrier in the entrance channel  $\text{CO} + \text{OH} \rightarrow \text{HOCO}^*$  and also in the exit channel  $\text{HOCO}^* \rightarrow \text{H} + \text{CO}_2$ . There is a large H-tunneling effect in the latter, and at low temperatures there is even tunneling in the former. In the Arrhenius plot of  $\ln k_{\text{rate}}$  vs  $1/T$  the slope increases significantly at temperatures higher than 500 K, reflecting the actual energy barrier that exists when H-tunneling becomes less important.

In a novel experiment Dreier and Wolfrum<sup>32</sup> formed vibrationally excited CO molecules by collision of CO with vibrationally excited  $\text{N}_2$ . The latter was obtained by microwave discharge in an  $\text{N}_2/\text{Ar}$  mixture to form excited  $\text{N}(^4S)$ , which then reacted with NO. The vibrational temperature  $T_v$  of the CO molecules was determined from the optical absorption spectrum of the vibrational-rotational states of  $\text{CO}(v, J)$  at or below 1800 K. On the other hand, the rotational and translational temperatures remained at room tem-

perature. The OH radicals were obtained from a discharge in  $\text{H}_2/\text{Ar}$  to yield H, which then further reacted with  $\text{NO}_2$  to form OH.

Under these conditions the rate constant appeared to decrease by about 15% from its room-temperature value when  $T_v$  was increased to 1800 K, though with large error bars (the results of many measurements). We treat this behavior in the present article and make predictions for  $v$  state-selected experiments, where the effects would be considerably larger.

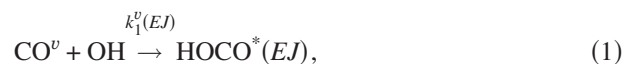
The calculational method is summarized in Sec. II, and the results are given and discussed in Sec. III.

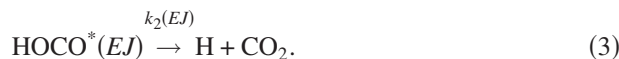
## II. THEORY AND CALCULATION METHOD

The key aspects of the calculations are noted below, with more details being given in the earlier paper.<sup>28</sup>

### A. Kinetic scheme and rate constants

Because the energy barrier between *cis*- and *trans*-HOCO is much lower than the energy barriers in the entrance and exit channels, we can assume as before that the *cis* and *trans* energetic intermediates HOCO\* easily interconvert. The pressure in the experiments was about 4 mbars,<sup>32</sup> and so collisional stabilization by bath gases can be neglected. At zero pressure, the kinetic scheme for the vibrationally excited CO molecules reacting with the OH radicals at an energy  $E$  and total angular momentum  $J$  is given by

<sup>a)</sup>Electronic mail: ram@caltech.edu



The rate constant for the forward reaction in Eq. (1) is denoted by  $k_1^v(EJ)$  when the CO vibration is initially in the quantum state  $v$ . The rate constant  $k_{-1}(EJ)$  in Eq. (2) yields CO having any CO vibrational quantum number and not necessarily having the initial  $v$ . The rate constants  $k_1^v(EJ)$ ,  $k_{-1}(EJ)$ , and  $k_2(EJ)$  are  $E$  and  $J$  dependent. The limiting low-pressure steady-state rate constant  $k^v$  for any specified initial CO vibrational quantum state  $v$  is given by

$$k^v = \sum_J \int_E \frac{k_1^v(EJ)k_2(EJ)}{k_{-1}(EJ) + k_2(EJ)} dE. \quad (4)$$

In terms of numbers of quantum states of the two transition states, this low-pressure rate constant at any given  $v$  is

$$k^v = \sum_J \int_E \frac{N_1^v(EJ)N_2(EJ)}{hQ[N_1(EJ) + N_2(EJ)]} dE, \quad (5)$$

where  $Q$  is the partition function of the OH and CO when CO is in the specified initial vibrational state  $v$ .  $N_1^v(EJ)$ ,  $N_1(EJ)$ , and  $N_2(EJ)$  denote the sums of quantum states of the transition states for the entrance at specified  $v$ , entrance at all accessible  $v$ 's, and exit channels, respectively, for the energy  $E$  and total angular momentum  $J$ . When  $v \geq 1$  the  $N_1(EJ)$  for the backward reaction in the entrance channel is larger than  $N_1^v(EJ)$  because the energy redistribution in the intermediate  $\text{HOCO}^*$  yields a large number of quantum states in  $N_1(EJ)$ . Each sum of states includes a tunneling correction for a microcanonical ensemble<sup>33,34</sup>

$$N_i(EJ) = \int_{E_{\min}}^E \kappa_i(E') \rho_i((E-E')J) dE' \quad (i=1,2) \quad (6)$$

and

$$N_1^v(EJ) = \int_{E_{\min}}^E \kappa_1(E') \rho_1^v((E-E')J) dE', \quad (7)$$

where  $E_{\min}$  denotes the energy minimum in  $\text{HOCO}^*$ . In Eq. (7) for  $N_1^v(EJ)$ , unlike Eq. (7) for  $N_1(EJ)$  and  $N_2(EJ)$ , only an energy  $E - v h \nu$  is available for energy redistribution in the  $\rho_1^v$  in this transition state: We note that for the  $E$  in  $N_1^v(EJ)$  in Eq. (7) one writes  $E - v h \nu$ .  $\kappa_i(E')$  is the tunneling transmission probability at an energy  $E'$  in the tunneling coordinate. As in Ref. 28,  $\kappa_i$  is estimated by tunneling through a fitted Eckart potential, and  $\rho_i((E-E')J)$  denotes the density of rovibrational states of the transition state  $i$  at an energy  $E - E'$  and total angular momentum  $J$ .

The rate constant at the vibrational temperature  $T_v$  is then given by

$$k(T_v) = \frac{1}{Q_{\text{CO}}^{\text{vib}}(T_v)} \sum_v k^v \exp\left(\frac{-v h \nu}{k_B T_v}\right), \quad (8)$$

where  $Q_{\text{CO}}^{\text{vib}}$  is the vibrational partition function of the CO molecules at a vibrational temperature  $T_v$ .

The potential-energy surface used is the same as that employed in the earlier paper,<sup>28</sup> with the same two adjusted parameters and the same refined vibrational frequencies of

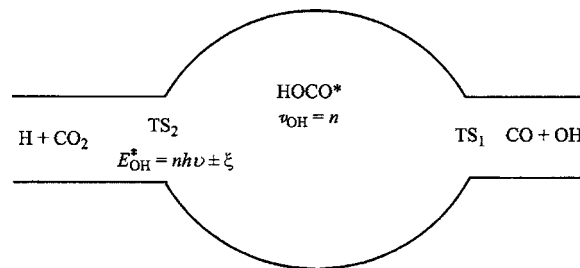


FIG. 1. Formation of CO+OH from H+CO<sub>2</sub>. All  $n$ 's are possible but the difference in energy in the OH coordinate between TS<sub>2</sub> and HOCO<sup>\*</sup> is  $\pm \xi$ . In TS<sub>2</sub> the OH bond stretching energy is  $nh\nu \pm \xi$ . In HOCO<sup>\*</sup> it is  $nh\nu$  for each  $n$ .

all stationary structures. In the calculation the number of quantum states of the internal rotation about the HO–CO bond in the entrance channel was treated as before as a one-dimensional hindered rotor.

## B. Nonstatistical modification of RRKM

We recall previous studies where the reaction CO+OH  $\rightarrow$  CO<sub>2</sub>+H showed a nonstatistical behavior<sup>35–40</sup> in both bulk gas-phase and molecular-beam studies of the reverse reaction, H+CO<sub>2</sub> $\rightarrow$ OH+CO. It was observed that the vibrational excitation of the CO product of that reaction was below that expected from statistical theory for the HOCO<sup>\*</sup> intermediate. There appear to be various nonstatistical components. In the present nonstatistical modification of the Rice-Ramsperger-Kassel-Marcus (RRKM) theory, as in Ref. 28, we simply assume that the intramolecular energy transfer between the high-frequency OH-stretching vibration in the HOCO<sup>\*</sup> and the other (lower-frequency) modes is not rapid enough to yield an intramolecular statistical distribution during the typical lifetime of the HOCO<sup>\*</sup> before the latter dissociates into H+CO<sub>2</sub>.

In our earlier study<sup>28</sup> a nonstatistical modification of the RRKM theory was also used to treat the reaction, a treatment which included H- and C-isotope effects. The nonstatistical modification removed an existing discrepancy in the literature<sup>26,41</sup> between results of experiment and the RRKM theory for the H-/D-isotope effect at low pressures. It reproduced the non-Arrhenius behavior for the rate constants at high and low temperatures.

In this nonstatistical modification<sup>28</sup> of the RRKM theory, it was assumed that only a limited amount of energy  $\xi$  can be transferred into or out of the OH-stretching vibration just before the HOCO<sup>\*</sup> enters the transition state TS<sub>2</sub>, from which it dissociates into H+CO<sub>2</sub>. That is, there is restricted energy transfer between the HOCO<sup>\*</sup> phase space and the phase space of TS<sub>2</sub>, as depicted schematically in Fig. 1 for the reverse reaction. The value assumed<sup>28</sup> for  $\xi$ , 4000 cm<sup>-1</sup>, is a little larger than the energy of one OH-stretching quantum. Therefore, the amount of energy in the H-dissociation motion in the TS<sub>2</sub> produced from an intermediate HOCO<sup>\*</sup> with  $n$  quanta in the OH vibration is limited in TS<sub>2</sub> to an energy in  $nh\nu \pm \xi$  interval, as shown in Fig. 2. The dissociation rate constant  $k_2(EJ)$  at a total energy  $E$  and angular momentum  $J$  of HOCO<sup>\*</sup> thus includes a partitioning over the quantum number  $n$  of the OH-stretching vibration in

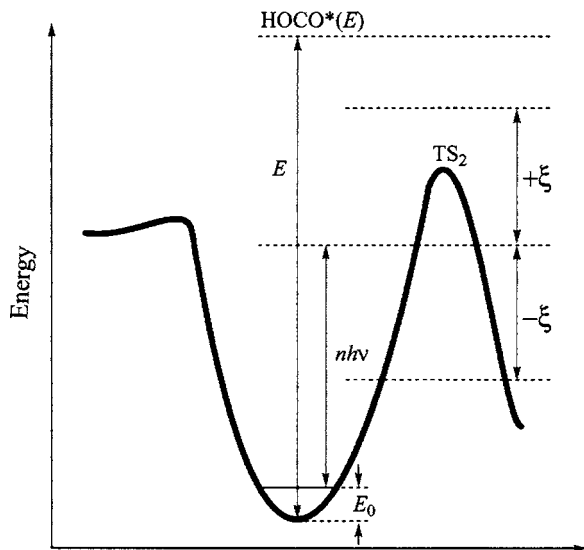


FIG. 2. Schematic profile of the relation between the HOCO\* with total energy  $E$  including  $n$  quanta in the OH stretching and the OH energy interval  $nh\nu \pm \xi$ , permitting the entrance into  $TS_2$  in the nonstatistical model.

HOCO\*. The allowed values of  $n$  are  $0, 1, \dots, n_{\max}$ , a total of  $(n_{\max} + 1)$  values, where  $n_{\max}$  is the maximum allowed quantum number of the OH-stretching vibration in the HOCO\* at the given  $E$  and  $J$ . The  $N_2(EJ)$  in Eq. (5) is thus replaced by the weighted sum,

$$N_2^{\text{non}}(EJ) = \frac{1}{(n_{\max} + 1)} \sum_{n=0}^{n_{\max}} N_2^n(EJ), \quad (9)$$

where in virtue of the definition of  $\xi$  we have

$$N_2^n(EJ) = \int_{\max[E_0 + nh\nu - \xi, E_0]}^{\min[E_0 + nh\nu + \xi, E]} \kappa_2(E') \rho_2((E - E')J) dE'. \quad (10)$$

The  $\kappa_2(E')$  and  $\rho_2((E - E')J)$  are the same as those in Eq. (6),  $\nu$  in Eq. (10) is the OH-stretching frequency of *cis*-HOCO, and the lower and upper bounds of  $E$  are as indicated.  $E_0$  is the potential energy plus the zero-point energy in HOCO\*. The upper and lower bounds of  $E$  in Eq. (10) limit the amount of energy  $\xi$  transferring between other modes and the OH-stretching motion in  $TS_2$ . When  $\xi$  approaches infinity, the energy transfer between modes is much faster than the lifetime of intermediates and the number of states used in the conventional RRKM is obtained at any  $n$ , i.e.,  $N_2^n(EJ) = N_2(EJ)$ .

Using Eq. (9) and the rate constants  $k_2^n(EJ)$  for the reaction from the intermediate HOCO\* with  $n$  quanta in the OH-stretching mode, the conventional RRKM rate constant at specified  $E$  and  $J$  can be expanded as

$$k(EJ) = \frac{N_2(EJ)}{h\rho(EJ)} = \frac{1}{n_{\max} + 1} \sum_0^{n_{\max}} \frac{\rho^n(EJ)}{\rho(EJ)} k_2^n(EJ), \quad (11)$$

since  $k_n(EJ) = N_2^n(EJ)/h\rho^n(EJ)$ , where  $\rho^n(EJ)$  is the density of states of the HOCO\* at OH vibrational state  $n$ . Equation (11) is Eq. (C3) (Ref. 42) in Ref. 28. The rate constant with nonstatistical modification can be obtained by using Eqs. (10) and (11) with a finite value of  $\xi$ .

TABLE I. The rate constants at the CO vibrational quantum number  $\nu$  at 298 K. The unit is  $10^{-13} \text{ cm}^3 \text{ molecule}^{-1} \text{ s}^{-1}$ .

$\nu$	RRKM	Nonstatistical	$K_{\text{non}}^{\nu}/K_{\text{RRKM}}^{\nu}$	Expt. (Ref. 32)
$\nu=0$	1.49	1.53	1.03	...
$\nu=1$	0.97	0.54	0.56	...
$\nu=2$	1.50	0.96	0.64	...
$\nu=3$	2.16	1.21	0.56	...
$\nu=4$	2.96	1.48	0.50	...
$k_{\text{total}}(T_v=298 \text{ K})$	1.49	1.53		$1.51 \pm 0.6$
$k_{\text{total}}(T_v=1400 \text{ K})$	1.44	1.42		$1.36 \pm 0.5$
$k_{\text{total}}(T_v=1800 \text{ K})$	1.41	1.37		$1.30 \pm 0.5$

### III. RESULTS AND DISCUSSION

The calculated rate constants are listed in Table I as a function of the initial CO vibrational quantum state  $\nu$ . In the RRKM theory and the nonstatistical modification, the rate constant first decreases by about factors of 1.5 and 3, respectively, on going from  $\nu=0$  to  $\nu=1$  and then increases with further increase in  $\nu$ . It is seen that  $\nu$  state-selected experiments, particularly  $\nu=0$  and 1, would be helpful in clarifying the importance of nonstatistical effects in the reaction.

This calculated dependence of the rate constants on  $\nu$  can be understood as follows: When  $\nu=0$  at 298 K we have  $N_1(EJ) > N_2(EJ)$  for a typical  $E$  (about  $500 \text{ cm}^{-1}$  at room temperature for  $\nu=0$ ) and  $J$ , as seen in Fig. 3, because the effective barrier in the exit channel is slightly higher than that in the entrance channel. That is, the low-pressure reaction-rate constant in Eq. (5) has its main bottleneck in the exit channel transition state. We also have  $N_1^{\nu=0}(EJ) \approx N_1(EJ)$  since very few CO's are vibrationally excited in returning to CO+OH via the entrance channel transition state  $TS_1$ . We note next that integration over  $E$  for any  $\nu$  begins at  $E = \nu h\nu$ , i.e., it is an integration over  $E'$  from 0 to  $\infty$ , where  $E' = E - \nu h\nu$ . When  $\nu=1$ ,  $N_1^{\nu=1}(EJ)$  is about equal to

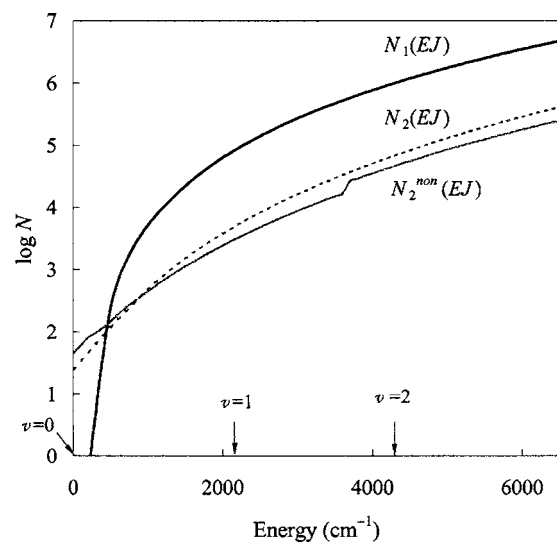


FIG. 3. The sums of states  $N_1(EJ)$ ,  $N_2(EJ)$ , and  $N_2^{\text{non}}(EJ)$  are plotted vs.  $E$ . The chosen  $J$  state shown on this plot is the most probable  $J$  at room temperature. The plots of  $N_1^{\nu=0}(EJ)$  and of  $N_1(EJ)$  overlap in the energy range at current interest. The vibrational energy of CO at  $\nu=1, 2$  is indicated in the abscissa. In  $N_2^{\text{non}}(EJ)$  the bump around  $3600 \text{ cm}^{-1}$  is due to the increase of accessible OH-vibrational states in  $N_2^{\text{non}}(EJ)$ .

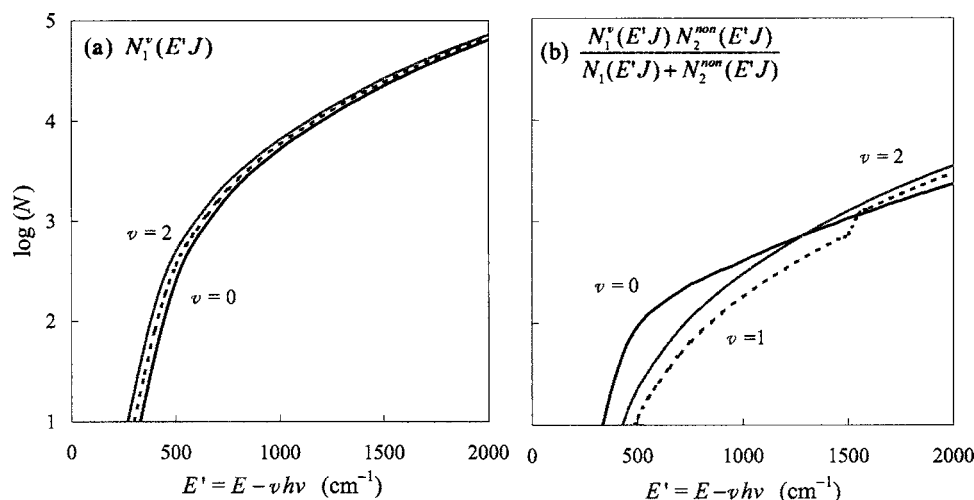


FIG. 4. The sums of states  $N_1^v(E'J)$  and  $[N_1^v(E'J)N_2^{\text{non}}(E'J)]/[N_1(E'J) + N_2^{\text{non}}(E'J)]$  obtained with the non-statistical theory are plotted vs  $E'$ , total energy  $E$  minus  $v h \nu$  at the specified  $v$ . The solid black, dotted black, and the solid gray lines denote the plots for  $v=0, 1$ , and  $2$ , respectively. The chosen  $J$  state shown on this plot is the most probable  $J$  at room temperature. In (b) the small bump for  $v=1$  around  $1500 \text{ cm}^{-1}$  is due to the increase of accessible OH-vibrational states in  $N_2^{\text{non}}(EJ)$ .

$N_1^{v=0}((E-h\nu)J)$ , as seen in Fig. 4(a), but  $N_1(EJ)$  and  $N_2(EJ)$  are enhanced significantly over their values at  $E-h\nu$ . The increase in  $N_1(EJ)$  is larger than that in  $N_2(EJ)$ , as seen in Fig. 3, because much of the energy in  $\text{TS}_2$  goes into overcoming the need for tunneling rather than only in increasing the number of quantum states. Thereby, the key quantity in Eq. (5),  $[N_1^v N_2]/[N_1 + N_2]$ , decreases when  $v$  is increased from 0 to 1, as seen in Fig. 4(b). At higher  $v$ , and hence higher energies,  $N_2(EJ)$  increases with  $E$  more rapidly than does  $N_1(EJ)$  (Fig. 5), perhaps because  $\text{TS}_1$  has more rotations (hindered) than  $\text{TS}_2$ , and the number of quantum states increases less rapidly for rotations (one squared term per coordinate) than for vibrations (two squared terms per coordinate). Thus, for  $v=1, 2, \dots$ , the ratio  $N_2(EJ)/[N_1(EJ) + N_2(EJ)]$  increases with energy (Fig. 5), and so the rate constants also increase with increasing  $v$ .

The present calculated result for  $v=1$  compared with  $v$

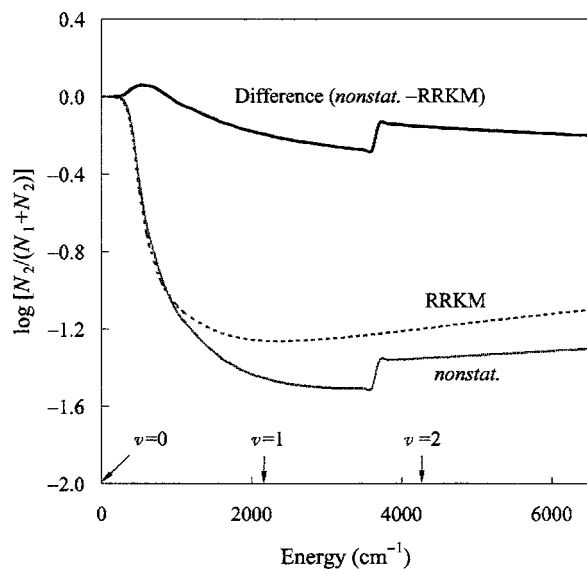


FIG. 5. Sums of states  $N_2(EJ)/[N_1(EJ) + N_2(EJ)]$  are plotted vs  $E$  at typical  $J$ . In nonstatistical calculations  $N_2^{\text{non}}(EJ)$  is used instead of  $N_2(EJ)$ . The difference is the value obtained with the nonstatistical modification minus that with the RRKM theory. The vibrational energy of CO at  $v=1, 2$  is indicated in the abscissa. In the nonstatistical calculations and the difference, the small bump around  $3600 \text{ cm}^{-1}$  is due to the increase of accessible OH-vibrational states in  $N_2^{\text{non}}(EJ)$ .

$=0$  is different from the classical trajectory results of Lakin *et al.*,<sup>23</sup> but the trend from  $v=1$  to  $v=2$  is in the same direction: Their calculation showed a cross section for the reaction that increased monotonically when  $v$  was increased from 0 to 2. The difference may have several origins, one being the absence of the quantum-mechanical tunneling in the exit channel transition state when classical trajectories are used. The consequences of this tunneling effect produce the decrease in  $k^v$  on going from  $v=0$  to  $v=1$ .

Because of the limited amount of internal energy transfer in the exit channel in the nonstatistical model [Eqs. (9) and (10)], the energy dependence of  $N_2^{\text{non}}(EJ)$  is smaller than that of  $N_2(EJ)$  of the RRKM theory. Thereby, the nonstatistical model has a weaker energy dependence of  $[N_1^v N_2^{\text{non}}]/[N_1 + N_2^{\text{non}}]$  on  $v$ , and so the enhancement of  $N_2^{\text{non}}(EJ)$  noted above with increase in  $v$  is less than that of  $N_2(EJ)$ , as seen in Fig. 3, and so the decrease in the  $k^v$  value from  $v=0$  to  $v=1$  is larger.

Since the calculated  $k^{v=1}$  value is smaller than  $k^{v=0}$ , the rate constants at higher vibrational temperatures are lower than the value at room temperature for the vibrational temperatures studied, 298, 1400, and 1800 K, as seen in Fig. 6. In the experiment<sup>32</sup> the rate constant in this range of  $T_v$ 's is smaller than the room-temperature value by 10% at 1400 K and 15% at 1800 K (but with large error bars). The calculated rate constants at the two temperatures,  $k_{\text{total}}(T_v=1400)$  and  $k_{\text{total}}(T_v=1800)$ , are lower than  $k_{\text{total}}(T_v=298)$  by 7% and 12%, respectively, in the modified statistical theory and by 3% and 5% in the unmodified RRKM theory. The trend is seen in Fig. 6.

We also note that quantum-mechanical calculations or perhaps classical trajectories can test the validity of the simple nonstatistical model assumed in Fig. 2. In passing we also note one property seen in Fig. 3 not needed in the discussion of the effect of  $v$  at room temperature but of interest at low temperature: At energies below  $\sim 300 \text{ cm}^{-1}$  we have  $N_1 < N_2$ . Its origin is that although the barrier at  $\text{TS}_2$  is somewhat higher than at  $\text{TS}_1$  there is so much tunneling at  $\text{TS}_2$  that the bottleneck at these low energies now occurs at  $\text{TS}_1$ , i.e.,  $N_1 < N_2$ .

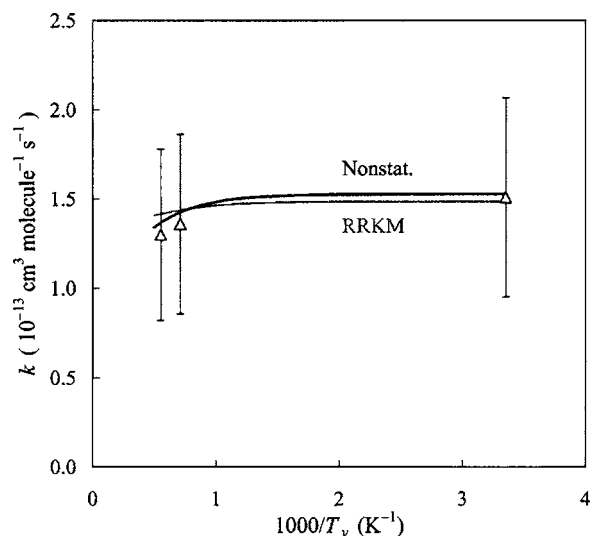


FIG. 6. Plot of rate constants vs CO-vibrational temperature  $T_v$ . The temperature for the other coordinates is 298 K. The calculated rate constants obtained with the RRKM theory and with the nonstatistical modification are shown by the gray and black lines, respectively. The open triangles and error bars are taken from the experimental data of Dreier and Wolfrum (Ref. 32).

#### IV. CONCLUSIONS

Both the RRKM and the nonstatistical modified theory yield a decrease in rate constant for the  $\text{OH} + \text{CO} \rightarrow \text{H} + \text{CO}_2$  reaction at higher CO-vibrational temperatures. Because of the limited energy transfer rate in the nonstatistically modified theory, the effect is stronger in the modified theory than in the standard RRKM theory and is also closer to the apparent experimental results.<sup>32</sup> State-selected experiments as a function of  $v$  are predicted (Table I) to first decrease and then increase with increasing  $v$  and, of course, yield much larger effects than vibrationally averaged results.

#### ACKNOWLEDGMENT

It is a pleasure to acknowledge the support of this research by the National Science Foundation.

- <sup>1</sup>R. P. Wayne, *Chemistry of Atmospheres*, 3rd ed. (Oxford University Press, New York, 2000).
- <sup>2</sup>A. Miyoshi, H. Matsui, and N. Washida, *J. Chem. Phys.* **100**, 3532 (1994).
- <sup>3</sup>C. D. Jonah, W. A. Mulac, and P. Zeglinski, *J. Phys. Chem.* **88**, 4100 (1984).
- <sup>4</sup>D. Fulle, H. F. Hamann, H. Hippler, and J. Troe, *J. Chem. Phys.* **105**, 983 (1996).
- <sup>5</sup>A. R. Ravishankara and R. L. Thompson, *Chem. Phys. Lett.* **99**, 377 (1983).
- <sup>6</sup>V. Lissianski, H. Yang, Z. Qin, M. R. Mueller, and K. S. Shin, *Chem. Phys. Lett.* **240**, 57 (1995).
- <sup>7</sup>M. S. Wooldridge, R. K. Hanson, and C. T. Bowman, *Int. J. Chem. Kinet.* **28**, 361 (1996).
- <sup>8</sup>M. S. Wooldridge, R. K. Hanson, and C. T. Bowman, *25th International Symposium on Combustion, University of California at Irvine, Irvine, CA,*

- 13 July-5 August 1994* (The Combustion Institute, Pittsburgh, PA, 1994), pp. 741–748.
- <sup>9</sup>T. A. Brabbs, F. E. Belles, and R. S. Brokaw, *13th International Symposium on Combustion, University of Utah, Salt Lake City, UT, 23–29 August 1970* (The Combustion Institute, Pittsburgh, PA, 1971), pp. 129–136.
- <sup>10</sup>M. J. Frost, P. Sharkey, and I. W. M. Smith, *J. Phys. Chem.* **97**, 12254 (1993).
- <sup>11</sup>M. J. Frost, P. Sharkey, and I. W. M. Smith, *Faraday Discuss. Chem. Soc.* **91**, 305 (1991).
- <sup>12</sup>A. J. Hynes, P. H. Wine, and A. R. Ravishankara, *J. Geophys. Res.* **91**, 11815 (1986).
- <sup>13</sup>A. Hofzumahaus and F. Stuhl, *Ber. Bunsenges. Phys. Chem.* **88**, 557 (1984).
- <sup>14</sup>R. Forster, M. Frost, D. Fulle, H. F. Hamann, H. Hippler, A. Schlepegrell, and J. Troe, *J. Chem. Phys.* **103**, 2949 (1995).
- <sup>15</sup>N. F. Scherer, C. Sipes, R. B. Bernstein, and A. H. Zewail, *J. Chem. Phys.* **92**, 5239 (1990).
- <sup>16</sup>D. M. Golden, G. P. Smith, A. B. McEwen, C. L. Yu, B. Eiteneer, M. Frenklach, G. L. Vaghjiani, A. R. Ravishankara, and F. P. Tully, *J. Phys. Chem. A* **102**, 8598 (1998).
- <sup>17</sup>H. G. Yu, J. T. Muckerman, and T. J. Sears, *Chem. Phys. Lett.* **349**, 547 (2001).
- <sup>18</sup>T. V. Duncan and C. E. Miller, *J. Chem. Phys.* **113**, 5138 (2000).
- <sup>19</sup>R. Valero and G. J. Kroes, *J. Chem. Phys.* **117**, 8736 (2002).
- <sup>20</sup>R. S. Zhu, E. G. W. Diau, M. C. Lin, and A. M. Mebel, *J. Phys. Chem. A* **105**, 11249 (2001).
- <sup>21</sup>J. P. Senosiain, C. B. Musgrave, and D. M. Golden, *Int. J. Chem. Kinet.* **35**, 464 (2003).
- <sup>22</sup>R. Valero, D. A. McCormack, and G. J. Kroes, *J. Chem. Phys.* **120**, 4263 (2004).
- <sup>23</sup>M. J. Lakin, D. Troya, G. C. Schatz, and L. B. Harding, *J. Chem. Phys.* **119**, 5848 (2003).
- <sup>24</sup>D. M. Medvedev, S. K. Gray, E. M. Goldfield, M. J. Lakin, D. Troya, and G. C. Schatz, *J. Chem. Phys.* **120**, 1231 (2004).
- <sup>25</sup>K. L. Feilberg, G. D. Billing, and M. S. Johnson, *J. Phys. Chem. A* **105**, 11171 (2001).
- <sup>26</sup>J. P. Senosiain, S. J. Klippenstein, and J. A. Miller, *Proc. Combust. Inst.* **30**, 945 (2005).
- <sup>27</sup>J. Troe, *Proceedings of the Combustion Institute*, **27**, 167 (1998).
- <sup>28</sup>W.-C. Chen and R. A. Marcus, *J. Chem. Phys.* **123**, 094307 (2005).
- <sup>29</sup>J. T. Petty, J. A. Harrison, and C. B. Moore, *J. Phys. Chem.* **97**, 11194 (1993).
- <sup>30</sup>J. Nolte, J. Grussdorf, E. Temps, and H. G. Wagner, *Z. Naturforsch., A: Phys. Sci.* **48**, 1234 (1993).
- <sup>31</sup>G. Poggi and J. S. Francisco, *J. Chem. Phys.* **120**, 5073 (2004).
- <sup>32</sup>D. Dreier and J. Wolfrum, *18th International Symposium on Combustion, University of Waterloo, Canada, 17–22 August 1980* (The Combustion Institute, Pittsburgh, PA, 1981), pp. 801–809.
- <sup>33</sup>R. A. Marcus, *J. Chem. Phys.* **45**, 2138 (1966).
- <sup>34</sup>W. H. Miller, *J. Am. Chem. Soc.* **101**, 6810 (1979).
- <sup>35</sup>J. K. Rice and A. P. Baronavski, *J. Chem. Phys.* **94**, 1106 (1991).
- <sup>36</sup>A. Jacobs, H. -R. Volpp, and J. Wolfrum, *Chem. Phys. Lett.* **218**, 51 (1994).
- <sup>37</sup>S. L. Nikolaisen, H. E. Cartland, and C. Wittig, *J. Chem. Phys.* **96**, 4378 (1992).
- <sup>38</sup>M. Brouard, D. W. Hughes, K. S. Kalogerakis, and J. P. Simons, *J. Phys. Chem. A* **102**, 9559 (1998).
- <sup>39</sup>M. Brouard, D. W. Hughes, K. S. Kalogerakis, and J. P. Simons, *J. Chem. Phys.* **112**, 4557 (2000).
- <sup>40</sup>M. Brouard, I. Burak, D. W. Hughes, K. S. Kalogerakis, J. P. Simons, and V. Stavros, *J. Chem. Phys.* **113**, 3173 (2000).
- <sup>41</sup>J. Troe, *Proc. Combust. Inst.* **30**, 952 (2005).
- <sup>42</sup>There is a typographical error in Eq. (C3) in Ref. 28. The denominator in the right-hand side of the equation should read  $(n_{\text{max}} + 1)$  instead of  $n_{\text{max}}$ .